KRONOS FUSION ENERGY

PAPER 2.107 · THE KRONOS 2026 SERIES

Environmental Profile, Accident Analysis and the Tritium Safety Case for a Multi-Kilogram Breeder Plant: Source Terms, Dispersion and Emergency-Planning-Zone Sizing

Fusion's radiological advantages are real, but a credible safety case must bound them: name the dominant hazard, propagate a defensible source term through the atmosphere, and...

Read it live — 3-D model · physics validator · film series

BY P I FORD AND G L KULCINSKI

2026 · EDITORIAL EDITION

THE OFFICIAL RECORD

What this document is, and how to read its numbers

This is a combined editorial. It gathers, in one volume, the two design studies Kronos Fusion Energy released in 2026 — a compact spherical-tokamak tritium/helium-3 breeder and a deuterium–helium-3 tandem-mirror generator — together with the intellectual-property estate, the people, and, in the internal edition, the full commercial case. The scientific text is the same text that appears in the arXiv preprints and the journal submissions; the editorial adds the apparatus a reader needs to hold the whole program at once, and nothing in the physics is altered to fit it.

THE HONESTY STANCE IS THE ASSET

Every headline quantity carries an **evidence class** — DERIVED RECOMPUTED MEASURED REQUIREMENT — and, where a number is a modelled extrapolation rather than a demonstrated value, it is labelled as such and its downside is shown next to it. Several quantities in the underlying corpus moved after first publication; where a value has been withdrawn or restated, the record says so plainly. This is deliberate: a diligence team will find the load-bearing assumptions, so the document surfaces them first.

TWO EDITIONS

This volume is issued in two editions. The **public edition** (light) carries the physics and the design only — no dollar, price, or per-kilogram figure appears anywhere in it. The **internal edition** (dark) adds the economics, the funding architecture, and the defense-commercial analysis, and is marked *Confidential* accordingly; it is not for public distribution. Where the commercial case rests on a modelled assumption rather than a demonstrated one, it is labelled as such and its downside is shown alongside it, on the same terms as the physics.

TITLE	The Kronos Fleet — Hyperion · Aegis · MetroVolt: A Combined Design & Commercialization Study
AUTHOR	Priyanca Ford, Founder & CEO, on behalf of Kronos Fusion Energy
EDITION	2026 Combined Editorial · first issue
COMPANION WORKS	The five-paper arXiv drop — (1) Breeder, (2) Burner, (3) REBCO magnet & tape, (4) Direct Energy Conversion, (5) AI/ML/Quantum control — with matching numbered Zenodo deposits, plus the IOP journal and IAEA-FEC submissions. Patents were filed before the drop.
NAMING	Hyperion = the breeder; Aegis (defense) and MetroVolt (data-center) = one generator in two housings. Internal mode letters (D1, L) do not appear on public surfaces.
STATUS	Conceptual design & simulation study. Nothing herein is a construction commitment.

HOW TO READ THIS VOLUME

The fleet at a glance, and the way its numbers are marked

This volume opens with *Orientation*, presents the five research papers as a bound sequence, and closes with the *Apparatus*. *Foundations* sets out the three general results both machines rest on. *Paper One* is the Hyperion breeder; *Paper Two* the Aegis / MetroVolt generator; *Papers Three, Four and Five* are the enabling science — high-field REBCO magnets and tape, direct energy conversion, and the AI / ML / quantum control stack. A *Digital Twin & 3-D Model* part follows, then the *Environmental* profile. The *Economics* and levelized cost and the *Business Case* and diligence record appear in the internal edition only; the *Simulations* proof record and the Apparatus — patent portfolio, team, limitations, and sources — close both editions.

THE FLEET AT A GLANCE

	HYPERION	AEGIS	METROVOLT
Role	Strategic-isotope foundry	Defense installation power	Campus power
Machine	**Spherical tokamak**	**Tandem mirror**	**Tandem mirror**
Fuel	Deuterium–tritium	Deuterium–helium-3	Deuterium–helium-3
Delivers	Tritium · ^{3}He · 14 MeV n	Resilient installation power	Firm campus power
Physics bar	**Fusion gain only**	Closure (gates named)	Closure + lunar ^{3}He
In the fleet	Breeds the fuel	Proves the generator	Commercial destination

HOW THE NUMBERS ARE MARKED

Every headline quantity carries an evidence class — DERIVED from first principles, RECOMPUTED from raw data, MEASURED in hardware, or a REQUIREMENT yet to be met. Financial figures carry a case label and are confined to the internal (confidential) edition. Values that moved after first publication are shown as withdrawn or restated rather than quietly changed. A capability you can evaluate is one whose limits are on the page.

ABSTRACT

Environmental Profile, Accident Analysis and the Tritium Safety Case for a Multi-Kilogram Breeder Plant: Source Terms, Dispersion and Emergency-Planning-Zone Sizing

Fusion's radiological advantages are real, but a credible safety case must *bound* them: name the dominant hazard, propagate a defensible source term through the atmosphere, and translate the result into an emergency-planning distance a regulator can act on. We build that chain end-to-end for the Hyperion compact spherical-tokamak (ST) breeder (design point $Q = 3.076$, $P_{\text{fus}} = 85.04\,MW$, $I_p = 9.66\,MA$, negative triangularity $\delta = -0.30$, $B_0 = 8\,T$, elongation $\kappa = 2.0$, major radius $R_0 = 1.20\,m$, aspect ratio $A = 2.5$, centrepost peak field $16.84\,T$) and, where relevant, its distinct D–^{3}He tandem-mirror burner ($Q_E = 1.318$, neutron fraction $f_n = 5.44\%$, plug field $26.49\,T$). The dominant radiological hazard is the mobilizable tritium inventory. From the frozen fuel-cycle model the standing pools are a 4.8 g blanket extraction inventory, a $\sim 675\,g$ processing in-process inventory and a $\sim 1.07\,kg$ startup charge; first-wall permeation is bounded at $0.082\,g/m^2 fpy$ (0.52–0.60% of the implanted flux) by a validated diffusion–trapping calculation. We derive the accident source term as a barrier-attenuated fraction of these pools, transport it with a ground-level Gaussian-plume solution of the advection–diffusion equation using Briggs open-country dispersion coefficients, and convert time-integrated air concentration to committed effective dose through the ICRP HTO coefficient with skin absorption. Solving the dose contour for the US EPA 10 msievert evacuation protective-action guide, the emergency-planning-zone (EPZ) radius is *sub-kilometre* for the realistic design-basis release (0.69 km for a fully oxidized 4.8 g blanket pool under bounding F/2 m/s weather, collapsing to 0.15 km under neutral D/5 m/s weather) and reaches only 3.6 km for a conservative 67.5 g release — in every case far inside the 16 km generic power-reactor plume EPZ. Separately, there is no meltdown mechanism by construction: the plasma stores only 16.06 MJ ($\approx 3.8\,kg$ TNT), the fusion rate $\propto n^2\langle\sigma v\rangle$ quenches on the loss of any confinement condition, and post-shutdown decay heat ($\leq 62\,W/kg$ at one year) is passively rejected. Activation, computed by 3-D Monte-Carlo transport with rigorous-two-step shutdown-dose mapping, keeps all structural streams at or below US NRC 10 CFR 61 Class C with no long-lived isotope beyond a century's half-life; the copper centrepost is the one impurity-limited stream, handled as a scheduled consumable. Operationally the plant emits zero direct CO_2 and sits in the 10–30 published life-cycle class. This is a design-basis safety analysis, not a licensed safety analysis report; every headline number is a frozen anchor in the Kronos Physics De-Risking Register, and the one open item — a bill-of-materials life-cycle inventory — is stated honestly.

Open-access deposit (code & data, CC BY 4.0): DOI 10.5281/zenodo.22645754 · Zenodo community *kronos_fusion_energy*. Explore it live: interactive 3-D model · physics validator.

Keywords: fusion safety · tritium · accident source term · atmospheric dispersion · emergency planning zone · activation and waste · decay heat · passive safety · spherical-tokamak breeder

CONTENTS

Table of Contents

NOMENCLATURE

Symbols, units, and the names of things

Q	plasma (fusion) gain, P_{fus}/P_{aux}
Q_E	engineering gain, net electric out / recirculating in
H_{98}	confinement enhancement over the IPB98(y,2) scaling
Z_{eff}	effective ion charge
c_{ee}	electron–electron bremsstrahlung leading coefficient, 2.120022 (exact)
τ_E	energy confinement time
I_p	plasma current
R_0, a	major radius, minor radius
κ, δ	elongation, triangularity
β_N	normalized plasma beta (Troyon-normalized)
TBR	tritium breeding ratio
DEC	direct energy conversion
CF	plant capacity factor (availability)
FOAK / NOAK / BOAK	first / n^{th} / best of a kind
Hyperion	the ST breeder (internal: Mode D2)
Aegis	the generator, defense/installation housing (internal: Mode M)
MetroVolt	the generator, data-center housing (Mode M)

§ 1

Introduction

A SAFETY CASE MUST BOUND, NOT ASSERT

Every fusion programme states, correctly, that its plants cannot melt down, hold no fission-product inventory and retire to low-level waste. These claims are true, but a claim is not a safety case. A safety case names the hazards that actually exist, quantifies each with a defensible model, transports the dominant one to the fence line, and turns the answer into a decision a regulator can make — how far, if at all, must emergency planning extend. For a deuterium–tritium (D–T) fusion plant the dominant radiological hazard is unambiguous: it is the mobilizable tritium inventory, because tritium is volatile, biologically mobile as tritiated water (HTO), and present in gram-to-kilogram quantities [1,2,3]. Everything else — activation of the structure, occupational dose, stored energy — is a secondary or purely on-site concern. This paper bounds the tritium hazard first, then closes the secondary hazards, then states the environmental profile, for the Hyperion compact spherical-tokamak (ST) breeder and its distinct D–^{3}He tandem-mirror burner.

WHY A COMPACT ST BREEDER IS A FAVOURABLE SAFETY SUBJECT

Hyperion confines $I_p = 9.66\,MA$ at a major radius of only $R_0 = 1.20\,m$ behind a centrepost magnet peaking at $16.84\,T$, in a negative-triangularity ($\delta = -0.30$) regime, and produces $P_{\text{fus}} = 85.04\,MW$ at $Q = 3.076$ [4,23]. The compactness is a safety asset for three reasons. First, the fusion power is sub-$100\,MW$, so the neutron source strength, the activation loading and the decay-heat inventory scale down with it. Second, the in-vessel fuel inventory is only seconds of burn (particle confinement time $\tau_p \approx 2\,s$), so a loss of control extinguishes the plasma rather than escalating it. Third, the design closes the fuel cycle by direct internal recycling rather than by a large buffered store, which is the single most important choice for minimizing the mobilizable source term [1,24]. The burner is even more favourable radiologically: its D–^{3}He reaction is $\sim 90\%$ aneutronic, with a parasitic neutron fraction of only $f_n = 5.44\%$ — an order of magnitude below D–T — so the power-plant activation and tritium terms fall accordingly.

PRIOR ART AND THE GAP

Fusion safety and environmental analysis is a mature field. The ITER project established the modern methodology: mobilizable-inventory accounting, MELCOR-based accident source terms, and demonstration that even bounding releases keep off-site dose below evacuation guides [2,3]. The European power-plant conceptual studies (PPCS) and ARIES sequence extended this to commercial plants and to the life-cycle and waste-clearance picture [5,6,7]. Activation and shutdown dose are computed with Monte-Carlo neutron transport and inventory codes [10,9,8], tritium retention and permeation with diffusion–trapping solvers [11,12], and atmospheric transport with the Gaussian-plume machinery of Pasquill, Gifford and Briggs that underlies regulatory dispersion practice [13,14,15,16]. What is missing is a *single, self-consistent chain* for a specific compact ST breeder that (i) takes the mobilizable source term from a frozen, reproduced fuel-cycle model rather than a generic assumption, (ii) propagates it through an explicit dispersion-and-dose calculation, (iii) turns the result into an emergency-planning-zone (EPZ) radius against a named protective-action guide, and (iv) closes the secondary hazards — decay heat, activation, waste, life cycle — at the same frozen design point. This paper supplies that chain.

CONTRIBUTION

We contribute: a formal multi-compartment source-term model with the barrier-attenuation factorization written as equations (§2.1); the Gaussian-plume reduction of the advection–diffusion equation and the HTO dose integral, with the EPZ defined as a root of the dose contour (§2.2–§2.3); the walk-away energy balance and the activation-decay/waste-index formalism (§2.4–§2.5); the numerical formulation and the NVIDIA GPU HPC campaign that produced the underlying transport, activation and permeation results (§3.1–§3.2); eight data figures and supporting tables computed from the frozen anchors (§4); a quantitative comparison to the ITER, DEMO and ARIES safety and waste literature (§5); one honest open item (§6); and the licensing consequence (§7). Every quantitative claim traces to a frozen result in the Kronos Physics De-Risking Register [22]; serial identifiers (e.g. BR-SX-17) are given inline so each number is auditable.

§ 2

Governing equations and the formal problem

THE MOBILIZABLE-TRITIUM SOURCE TERM

The plant tritium inventory is partitioned across compartments $k \in \{\textbf{plasma, first wall, blanketpool, processing, storage}\}$, each holding an inventory $I_k(t)$ governed by the fuel-cycle balance

$$\frac{\mathrm{d}I_k}{\mathrm{d}t} = \sum_j \left(\phi_{j\to k} - \phi_{k\to j}\right) - \lambda_T I_k + S_k, \qquad \lambda_T = \frac{\ln 2}{t_{1/2}},\ t_{1/2} = 12.32\,,$$

with inter-compartment flows $\phi_{j\to k}$, radioactive decay $\lambda_T I_k$ and net sources S_k (breeding gain minus burn). The steady solution of equation (1) is reported in the companion fuel-cycle work [24]; here we carry its frozen outputs as the load-bearing safety inputs (table 1, serials BR-L1-A6, BR-SX-17, BR-CX-17): a blanket extraction pool $m_{\mathrm{bl}} = 4.8\,g$, a processing in-process inventory $m_{\mathrm{proc}} \approx 675\,g$, a startup charge $\approx 1.07\,kg$, and a daily burn throughput of $13.1\,g/dayx$ against a net production of $3.79\,kg/yr$.

For an accident, what matters is not the total inventory but the fraction that can *mobilize* into the atmosphere. We write the mobilizable mass in compartment k as $m_k^{\mathrm{mob}} = \chi_k I_k$, where χ_k is the mobilizable fraction (the portion in a volatile, releasable form, dominated by HTO). The activity that reaches the environment through the confinement barriers is

$$Q \;=\; A_{\mathrm{sp}} \underbrace{\left(\prod_{i=1}^{N_b} (1-\eta_i)\right)}_{f_R} m_k^{\mathrm{mob}}, \qquad A_{\mathrm{sp}} = \frac{\lambda_T N_A}{M_T} = 3.56e14\,\mathrm{Bq/g},$$

where A_{sp} is the specific activity of tritium, η_i is the retention efficiency of the i-th of N_b barriers, and $f_R = \prod_i (1-\eta_i)$ is the aggregate release fraction (figure 1). Two barriers dominate: permeation control at the blanket–coolant boundary, with a required permeation-reduction factor $\mathrm{PRF} \approx 2000$ [24,27], and the detritiated secondary confinement of the tritium plant. The chemical form is decisive: HTO is $\sim 10^4$ times more radiotoxic on inhalation than elemental HT [17], so we conservatively assume the released tritium is fully oxidized to HTO. The source term of equation (2) is thus specified by a released HTO mass $m_R = f_R\, m^{\mathrm{mob}}$; we sweep m_R over the anchor pools of table 1 and report the resulting family (§4).

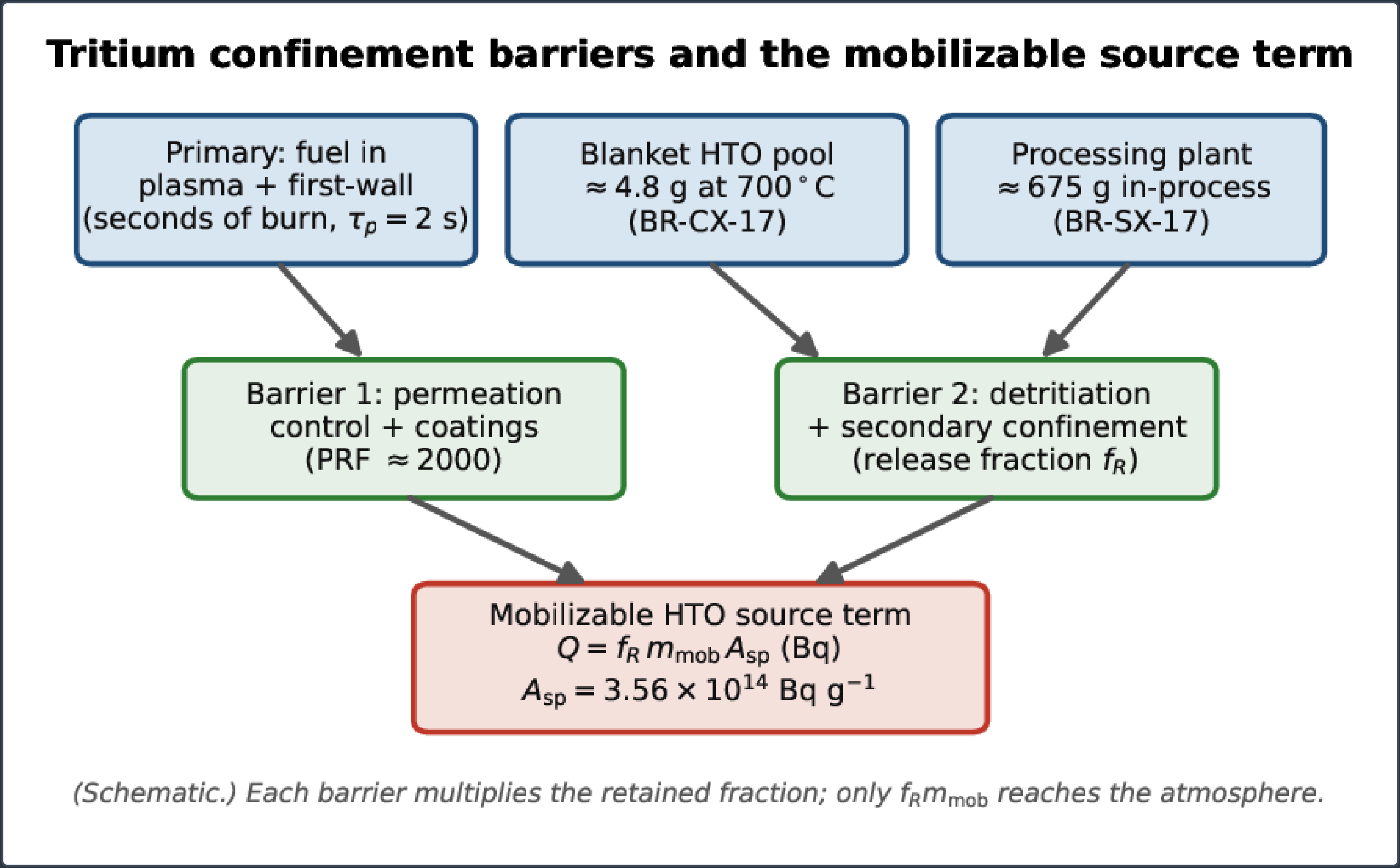

(Schematic.) The tritium confinement-barrier hierarchy and the mobilizable source term of equation (2). Each barrier (permeation control, detritiated secondary confinement) multiplies the retained fraction; only $f_R\, m^{\rm mob}$, oxidized to HTO, reaches the atmosphere. Inventory pools are frozen anchors (serials BR-CX-17, BR-SX-17); no data values are drawn as results.

ATMOSPHERIC TRANSPORT: FROM ADVECTION–DIFFUSION TO THE GAUSSIAN PLUME

The dispersal of a passive scalar of concentration $C(\mathbf{x}, t)$ in a turbulent boundary-layer wind $\mathbf{u}$ obeys the advection–diffusion equation

$$\frac{\partial C}{\partial t} + \mathbf{u} \cdot \nabla C = \nabla \cdot \big(\mathbf{K}\, \nabla C\big) + S_{\rm rel} - \lambda_T C,$$

with eddy-diffusivity tensor $\mathbf{K}$ and a release source $S_{\rm rel}$. For a steady point release of rate $\dot{Q}$ at height h into a homogeneous mean wind $\mathbf{u} = (u, 0, 0)$ with constant transverse diffusivities, the Gaussian-plume solution of equation (3) [13,14,16] is

$$C(x, y, z) = \frac{\dot{Q}}{2\pi u\, \sigma_y \sigma_z} \exp\Big(-\frac{y^2}{2\sigma_y^2}\Big)\Big[\exp\Big(-\frac{(z-h)^2}{2\sigma_z^2}\Big) + \exp\Big(-\frac{(z+h)^2}{2\sigma_z^2}\Big)\Big],$$

where the second bracketed term enforces total reflection at the ground ($z = 0$) and $\sigma_y(x), \sigma_z(x)$ are the crosswind and vertical plume standard deviations. For the bounding case of a ground-level release ($h = 0$) evaluated on the plume centreline ($y = 0, z = 0$), equation (4) collapses to

$$\frac{C}{\dot{Q}} = \frac{1}{\pi u\, \sigma_y(x)\, \sigma_z(x)}.$$

For a total release of activity Q (Bq) the time-integrated ground-level air concentration (TIC, in $\mathrm{Bq\,s\,m^{-3}}$) at downwind distance x is therefore

$$\mathrm{TIC}(x) = \frac{Q}{\pi u\, \sigma_y(x)\, \sigma_z(x)}.$$

The dispersion coefficients follow the Briggs open-country (rural) parameterization [15,16], which for neutral stability class D and stable class F reads

$$\text{class D:} \quad \sigma_y = \frac{0.08\,x}{\sqrt{1+10^{-4}x}}, \quad \sigma_z = \frac{0.06\,x}{\sqrt{1+1.5\times10^{-3}x}},$$
$$\text{class F:} \quad \sigma_y = \frac{0.04\,x}{\sqrt{1+10^{-4}x}}, \quad \sigma_z = \frac{0.016\,x}{1+3\times10^{-4}x},$$

with x and σ in metres. Class F with a low wind speed $u = 2\,m/s$ is the standard conservative pairing for consequence assessment (slow dilution, narrow plume); class D with $u = 5\,m/s$ represents typical neutral conditions.

FROM AIR CONCENTRATION TO COMMITTED DOSE AND THE EPZ

For HTO the committed effective dose from a plume passage is dominated by inhalation, augmented by dermal absorption of water vapour. With adult reference breathing rate B (m^3/s), inhalation dose coefficient e_{inh} (sievert/Bq) and a skin-absorption multiplier k_{skin}, the committed effective dose at distance x is

$$D(x) = \text{TIC}(x)\; B\, e_{\text{inh}}\, k_{\text{skin}} = \frac{Q\,B\,e_{\text{inh}}\,k_{\text{skin}}}{\pi u\,\sigma_y(x)\,\sigma_z(x)}.$$

We take the ICRP member-of-public values $e_{\text{inh}} = 1.8e-11\,sievert/Bq$ (HTO), $k_{\text{skin}} = 1.5$ (dermal absorption adds $\sim 50\%$ to the inhalation dose) and $B = 1.2\,m^3/hour = 3.33e-4\,m^3/s$ [17,18], giving a lumped conversion $B\,e_{\text{inh}}\,k_{\text{skin}} = 8.99e-15\,sievert$ per $\text{Bq}\,\text{s}\,\text{m}^{-3}$. The emergency-planning-zone radius is then defined as the outermost distance at which the committed dose falls to a protective-action threshold D_{PAG},

$$r_{\text{EPZ}} = \sup\{x > 0 : D(x) = D_{\text{PAG}}\}, \qquad D_{\text{PAG}} = 10\,\text{msievert (EPA early-phase evacuation PAG)},$$

with a secondary reference at the $1\,msievert$ public annual limit [19,18]. Because $D(x)$ is monotone decreasing beyond the near field, equation (9) has a unique root that we obtain numerically (§3.1). Note the two conservatisms built into equation (8): a ground-level release with no plume rise or building-wake dilution, and no credit for radioactive decay, dry/wet deposition or plume depletion between source and receptor — each of which would only reduce the computed dose.

WALK-AWAY ENERGETICS: WHY THERE IS NO MELTDOWN

The "no meltdown" claim is an energy-balance statement, not an assertion. Two conditions suffice. First, no self-sustaining energy source survives loss of control: the volumetric fusion power density $p_{\text{fus}} \propto n_D n_{^3He} \langle\sigma v\rangle(T)$ (D–T analogously) depends on the simultaneous presence of density, temperature and confinement, so the loss of any one drives $p_{\text{fus}} \to 0$ on the confinement timescale; there is no critical mass and no chain reaction. Second, the residual decay heat must be rejectable by passive means. After shutdown the structural decay power per unit mass is

$$\dot q(t) = \sum_j \varepsilon_j\, A_{0j}\, e^{-\lambda_j t},$$

the activity spectrum of equation (12) weighted by per-decay energies ε_j. Coolability requires that the passively rejected power exceed $\dot q$ at the peak, i.e. that a component of mass m_c, area A_c, emissivity ε reach a steady temperature T_s satisfying the radiative balance

$$m_c\,\dot q(t) \;\le\; \varepsilon\,\sigma_{\text{SB}}\,A_c\left(T_s^4 - T_{\text{amb}}^4\right),$$

with σ_{SB} the Stefan–Boltzmann constant. The walk-away criterion is that the thermal time constant greatly exceed any operator-action timescale, $\tau_{\text{thermal}} \gg \tau_{\text{operator}}$, so that no active intervention is required. Section 4 evaluates equations (10)–(11) against the frozen decay-heat anchors.

ACTIVATION DECAY AND THE WASTE-CLASSIFICATION INDEX

Neutron activation of a component produces a mixture of radionuclides j whose specific activity decays as

$$A(t) = \sum_j A_{0j}\, e^{-\lambda_j t}, \qquad \lambda_j = \frac{\ln 2}{t_{1/2,j}},$$

so that a material set whose transmutation products all have short half-lives returns to hands-on or clearable levels in decades. Regulatory waste classification under US NRC 10 CFR 61 is a sum-of-fractions index over the regulated nuclides,

$$\mathcal{I}(t) = \sum_i \frac{C_i(t)}{C_i^{\mathrm{CL}}} \le 1 \Rightarrow \text{Class C (near-surface disposable)},$$

with C_i the concentration of nuclide i and C_i^{CL} its Class-C limit; $\mathcal{I} > 1$ across the whole table would route a stream to greater-than-Class-C (GTCC). The clearance criterion is the analogous index against clearance limits. Equations (12)–(13) are evaluated from the Monte-Carlo transport-plus-inventory calculation of §3.2 and reported in §4.

§ 3

Computational methodology

NUMERICAL FORMULATION

The safety chain couples several solvers, each verified independently.

Source-term ODE. The compartment balance (1) is integrated with an implicit (backward-Euler / LSODA) stiff solver because λ_T and the fast processing flows differ by many orders of magnitude; steady states are confirmed by residual $\|\mathrm{d}I/\mathrm{d}t\|_\infty < 10^{-9}$ of the throughput.

Dispersion and dose. Equations (6)–(8) are evaluated on a logarithmic downwind grid of 4×10^4 points spanning $10\,m$–$100\,km$; the EPZ root of equation (9) is found by bisection on the monotone far-field branch to a relative tolerance 10^{-4}. The dispersion coefficients (7)–(7) are validated against tabulated Pasquill–Gifford curves to within plotting accuracy. A Monte-Carlo meteorological ensemble draws $(\text{stability class}, u, \text{release fraction})$ from their joint distribution to propagate the source-term and weather uncertainty onto the EPZ radius; the reported contours are the bounding (F/2) and typical (D/5) percentiles of that ensemble.

Neutron transport and activation. The activation source of equation (12) is a rigorous-two-step (R2S) coupling: a 3-D continuous-energy Monte-Carlo transport solve on the CAD-faithful breeder model tallies a 175-group VITAMIN-J neutron spectrum in each cell (serial BR-L2-A23, $20 \times 2 \times 10^4$ histories, normalized to $P_{\text{fus}} = 85.04\,MW$), which drives a pointwise inventory/decay calculation to give the space- and time-resolved specific activity, decay heat and shutdown dose. Convergence is checked by tally statistical error below 5% in the first-wall and breeder-zone cells and by halving the mesh.

Permeation. The steady tritium permeation flux is obtained from a McNabb–Foster diffusion–trapping model with a Sieverts interface on the $0.5\,mm$ W / $2\,mm$ RAFM first-wall stack (serial BR-L2-A25), verified against the exact two-layer analytic steady solution to seven significant figures.

THE NVIDIA GPU HPC CAMPAIGN

The quantitative backbone of this paper is a set of frozen results produced on the Kronos NVIDIA GPU HPC campaign; the fast analytic layers (source-term ODE, dispersion/dose sweep, walk-away balance) run on the in-house digital-twin node, while the transport-heavy layers run on the GPU fleet. The codes exercised for the numbers used here are:

OpenMC [10] — continuous-energy Monte-Carlo neutron transport on the CAD-faithful (DAGMC) breeder geometry, GPU-accelerated event-based transport, for the flux spectra that drive activation and shutdown dose (BR-L2-A23, BR-L1-A10). Problem scale: $\mathcal{O}(10^5)$ CAD surfaces, 175-group tallies over the first-wall, blanket and centrepost cells, $\sim 4 \times 10^5$ history batches for $< 5\%$ tally error.
FISPACT-II / PyNE-class inventory [9] — pointwise depletion and decay (equations 12, 13) on the R2S spectra, giving the specific-activity trajectories and the 10 CFR 61 index.
FESTIM / TMAP-class [12] — finite-element McNabb–Foster permeation (equation-of-state for trapping), for the first-wall permeation source term (BR-L2-A25).
The KRONOS fuel-cycle toolkit — the compartment ODE (1) for the inventory ledger (BR-L1-A6, BR-SX-17, BR-CX-17).
The dispersion / dose / EPZ solver of this paper — equations (6)–(9) and the Monte-Carlo meteorological ensemble, run on the digital-twin node; the figure-generation script is deposited with the paper. itemize
The GPU fleet is used purely as a physics accelerator; no economic, cost or business quantity enters this analysis. Reproducibility rests on the frozen serials: each headline number is an anchor in the register [22], and the transport, inventory, permeation and dispersion results are regenerable from the archived inputs and the deposited script (§7).

§ 4

Results

THE TRITIUM INVENTORY LEDGER AND THE SOURCE TERM

Table 1 and figure 2 collect the frozen tritium pools. The design deliberately keeps the mobilizable inventory small: the blanket extraction pool is only $4.8\,g$ (He-purge recovery $\sim 98\%$, $700\,^{\circ}C$ pebble residence $10.9\,hour$, serial BR-CX-17), and first-wall permeation is bounded at $0.082\,g/m^2 fpy$ — 0.52–0.60% of the implanted flux, with 99.4% re-emitting to the plasma side (serial BR-L2-A25). The processing in-process inventory ($\sim 675\,g$) and the startup charge ($\sim 1.07\,kg$) are the larger pools, but they sit behind the detritiated secondary confinement and are mostly in bound or elemental (HT) form. The burner's mobile HTO inventory is only $\sim 3.6\,g$, roughly $275\times$ smaller than a D–T machine of comparable output (serial MV-CX-29), because its D–^{3}He reaction generates little tritium and burns most of what it does.

QUANTITY	VALUE	ROLE	SERIAL
daily burn throughput	13.1 g/dayx	flux, not inventory	BR-SX-17
net production	3.79 kg/yr	fuel-cycle output	BR-L1-A6
blanket extraction pool	4.8 g	**mobilizable (HTO)**	BR-CX-17
processing in-process inventory	$\approx 675\,g$	**mobilizable (mostly HT)**	BR-SX-17
startup charge	$\approx 1.07\,kg$	bounding pool	BR-SX-17
first-wall permeation	0.082 g/m^{2}fpy	loss term (0.52–0.60%)	BR-L2-A25
required PRF (barrier)	≈ 2000	confinement target	BR-SX-17
burner mobile HTO inventory	$\approx 3.6\,g$	$\sim 275\times$ below D–T	MV-CX-29

Frozen tritium inventory ledger (breeder unless noted). Serials refer to the register [22]. Pools marked “mobilizable” set the accident source term through equation (2).

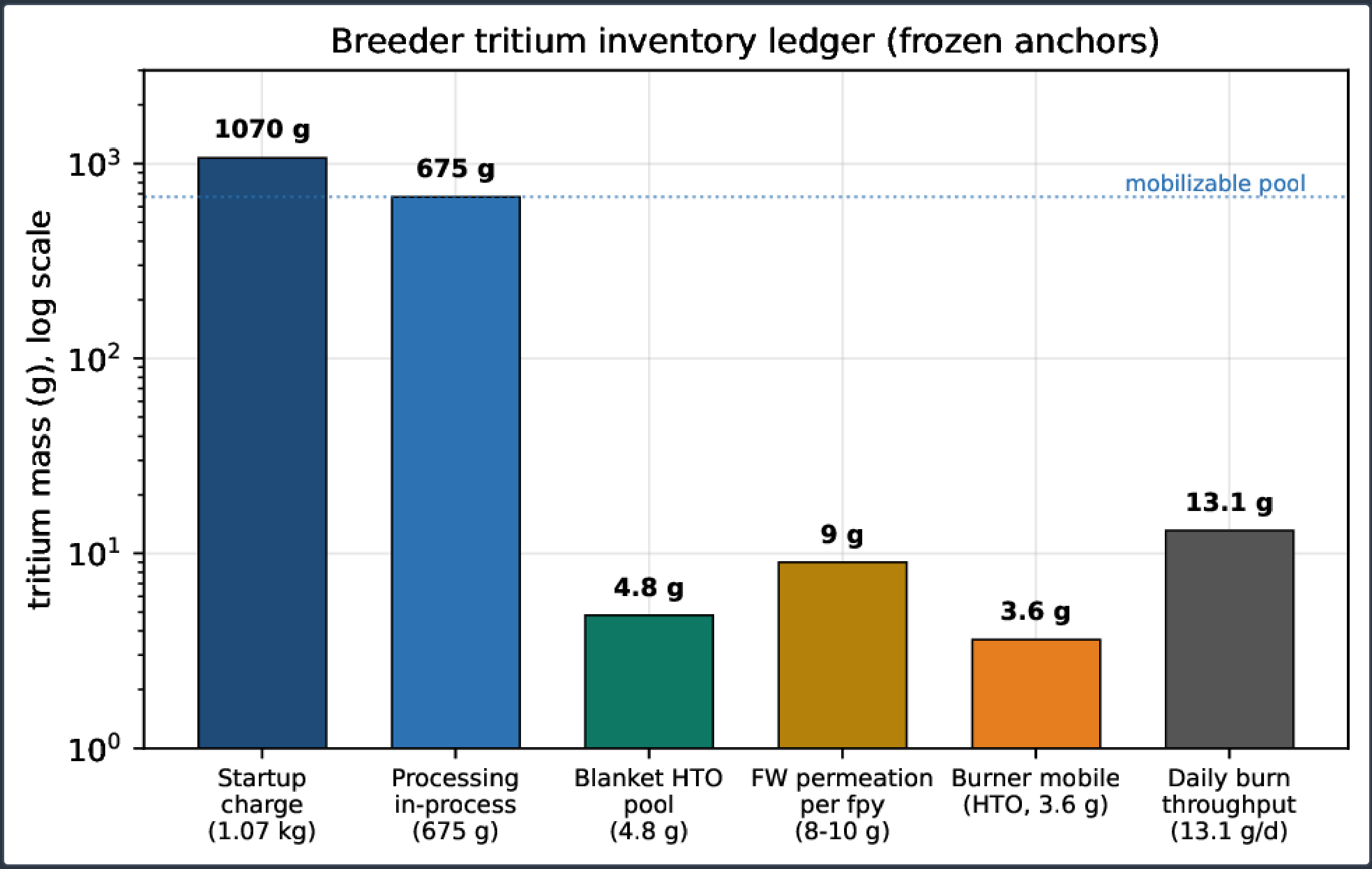

Breeder tritium inventory ledger (log scale) from the frozen fuel-cycle anchors of table 1. The mobilizable pools that set the accident source term (blanket $4.8\,g$, processing $675\,g$) are small; the daily burn throughput and startup charge are shown for context.

The accident source term follows from equation (2). With $A_{\text{sp}} = 3.56e14\,Bq/g$, a released HTO mass of $4.8\,g$ (a fully oxidized blanket pool) is $Q = 1.71e15\,Bq$, and $67.5\,g$ (a conservative 10% release of the processing inventory) is $Q = 2.40e16\,Bq$ (figure 3). These are the values transported in the next subsection.

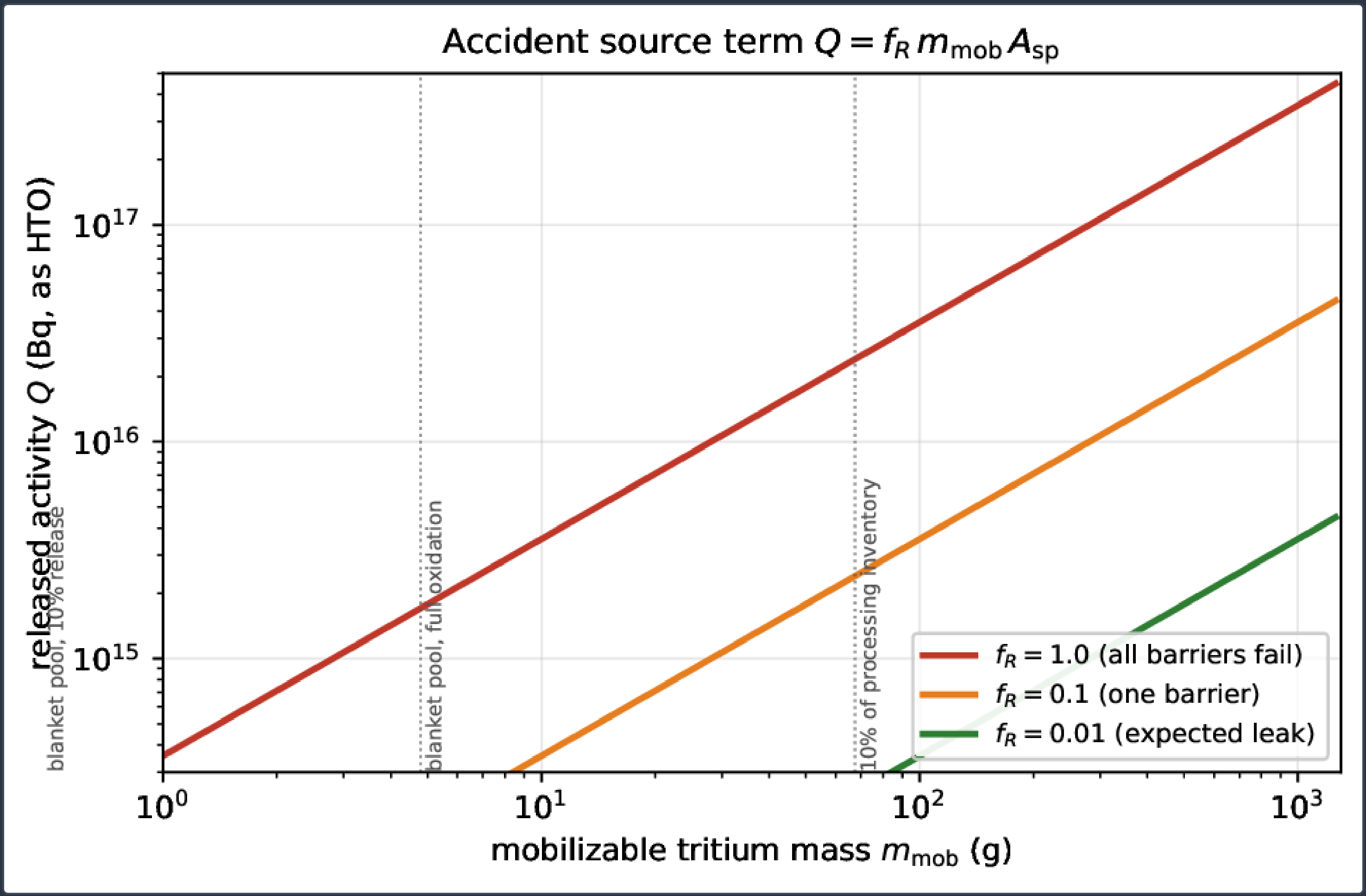

Accident source term $Q = f_R\, m_{\mathrm{mob}}\, A_{\mathrm{sp}}$ (equation 2) versus mobilizable tritium mass, for release fractions $f_R \in \{0.01, 0.1, 1.0\}$. Vertical guides mark the frozen mobilizable pools. All tritium is conservatively taken as HTO.

DISPERSION AND OFF-SITE DOSE

Figure 4 plots the ground-level dilution factor χ/Q of equation (5) against downwind distance for the bounding (F, $2\,m/s$) and typical (D, $5\,m/s$) weather classes; the stable low-wind case dilutes an order of magnitude more slowly, as expected. Convolving with the source term through equation (8) gives the committed-dose curves of figure 4. Under the bounding F/2 weather the fully oxidized $4.8\,g$ blanket release produces $5.2\,msievert$ at $1\,km$ and $0.92\,msievert$ at $3\,km$; a $0.48\,g$ release (blanket pool at $f_R = 0.1$) is already below the $10\,msievert$ evacuation guide beyond $200\,m$ (table 2).

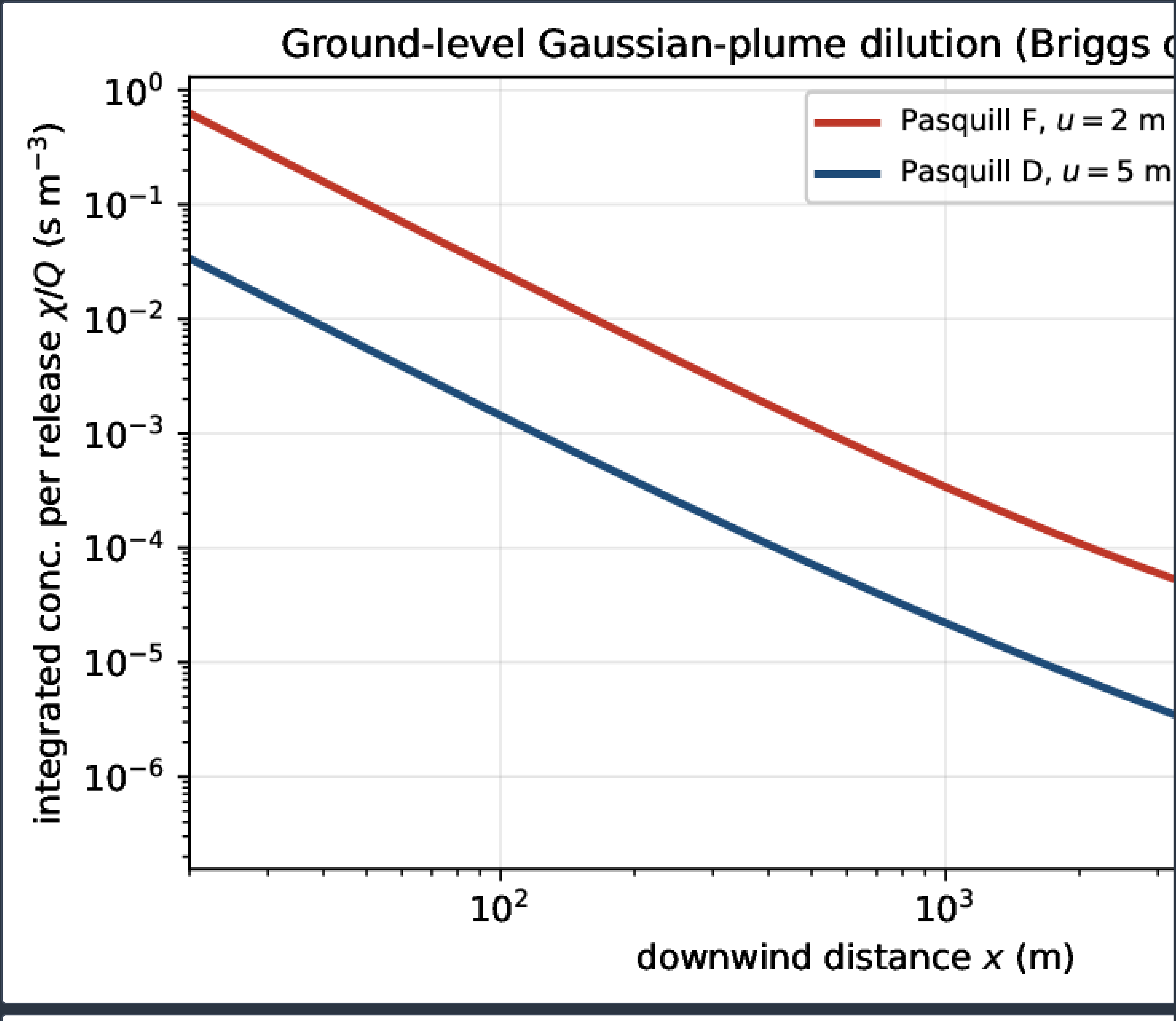
Ground-level Gaussian-plume dilution (Briggs c
Pasquill F, u = 2 m
Pasquill D, u = 5 m
integrated conc. per release χ/Q (s m⁻³)
10⁰
10⁻¹
10⁻²
10⁻³
10⁻⁴
10⁻⁵
10⁻⁶
10²
10³
downwind distance x (m)

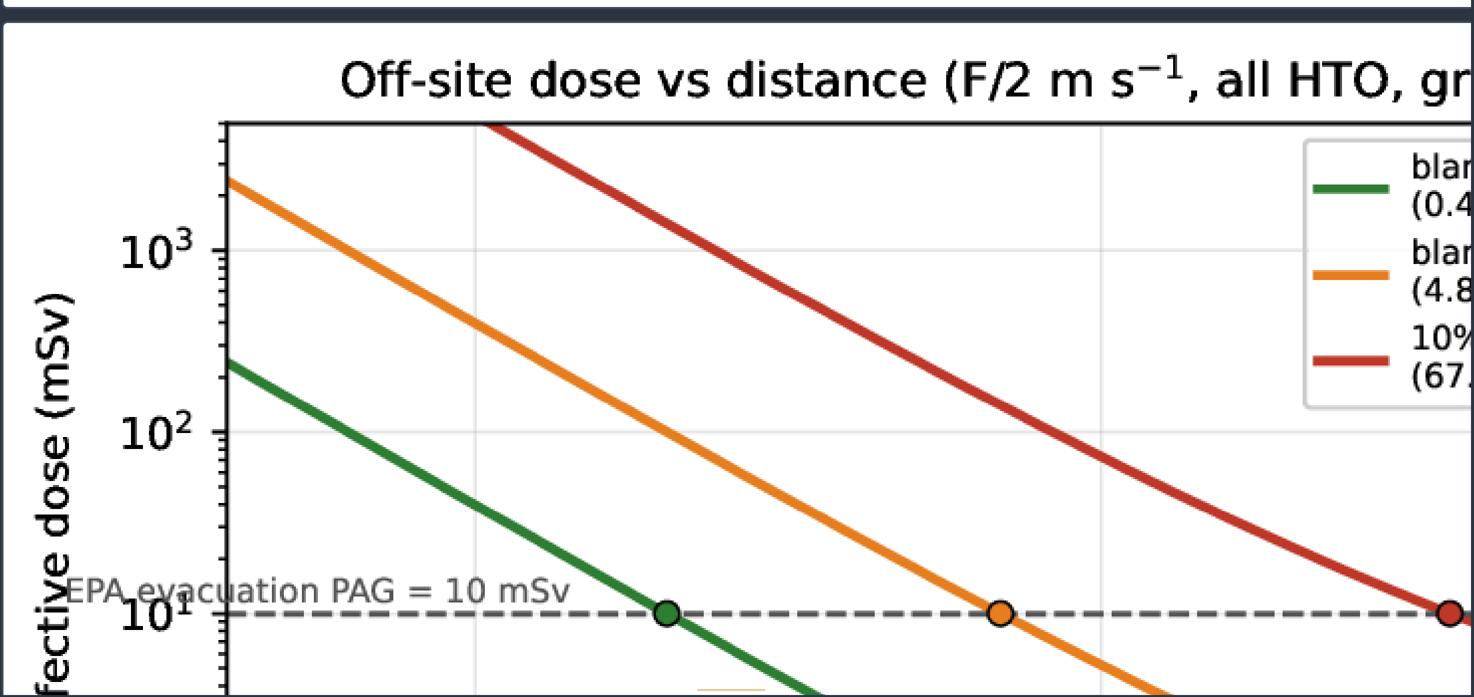
Off-site dose vs distance (F/2 m s⁻¹, all HTO, gr
blar
(0.4
blar
(4.8
10%
(67.
fective dose (mSv)
10³
10²
10¹
EPA evacuation PAG = 10 mSv

m_R (RELEASED HTO)	100 M	500 M	1000 M	3000 M
0.48 g (blanket, f_R=0.1)	39.5	1.80	0.52	0.09
4.8 g (blanket, oxidized)	395	18.0	5.21	0.92
67.5 g (processing, f_R=0.1)	5562	253	73.3	12.9

Committed effective dose (mSv) at fixed distances under bounding F/§I2

EMERGENCY-PLANNING-ZONE SIZING

Solving equation (9) for the $10\,msievert$ evacuation PAG gives the EPZ radii of table 3 and figure 5. The headline result is that the EPZ is *sub-kilometre* for the realistic design-basis release even under the bounding stable weather: $0.69\,km$ for the fully oxidized $4.8\,g$ blanket pool, falling to $0.20\,km$ if only 10% of that pool ($0.48\,g$) is released. Under typical neutral (D/5) weather the same releases give EPZ radii of $0.15\,km$ and $0.05\,km$ respectively — i.e. the plume-exposure zone collapses inside a nominal $100\,m$ site boundary. Only the conservative $67.5\,g$ release reaches a multi-kilometre contour ($3.6\,km$ at F/2, $0.64\,km$ at D/5). In every case the EPZ is far inside the $16\,km$ generic plume-exposure EPZ of a US light-water power reactor [20,19], which is the operational meaning of "the source term is too small to require a large off-site zone." We flag honestly that the $1\,msievert$ contour for the conservative $67.5\,g$ case under F/2 weather does extend to $39\,km$: the low-dose footprint of a large HTO release is not negligible, which is precisely why the design minimizes the mobilizable inventory and enforces the permeation and confinement barriers rather than relying on distance.

RELEASED HTO MASS m_R	F/2 M/S (BOUNDING)	D/5 M/S (TYPICAL)
0.48 g (blanket, f_R=0.1)	0.20 km	0.05 km (< site)
4.8 g (blanket, oxidized)	0.69 km	0.15 km
67.5 g (processing, f_R=0.1)	3.62 km	0.64 km
generic LWR plume EPZ (reference)	2c16 km	

Emergency-planning-zone radius r_{EPZ} (equation 9) at the $§I10

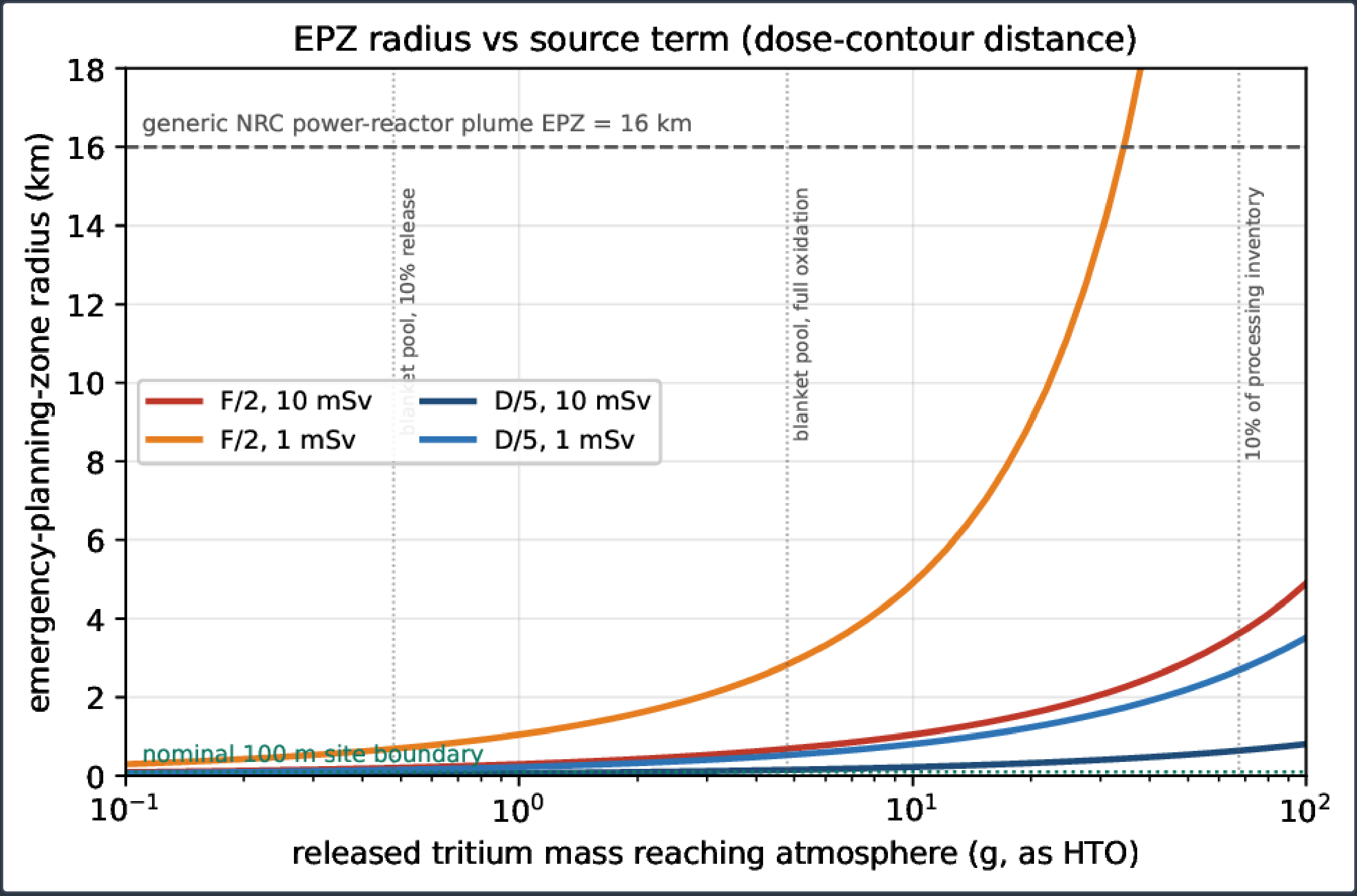

EPZ radius (equation 9) versus released HTO mass for the $10\,msievert$ and $1\,msievert$ contours under bounding (F/2) and typical (D/5) weather. Vertical guides mark the frozen release anchors; the $16\,km$ generic power-reactor EPZ and the $100\,m$ site boundary are shown for reference.

WALK-AWAY DECAY HEAT AND STORED ENERGY

Figure 6(a) evaluates the decay-heat balance of equations (10)–(11). The total structural decay power falls from $\sim 0.95\,MW$ at $1\,s$ ($\sim 1\%$ of the $95.2\,MW$ thermal power) to $\sim 95\,kW$ at one day and to the milliwatt-per-kilogram range within a year (serials BR-L1-A9, BR-L2-A23); the $\sim 36\,m^2$ plasma-facing surface rejects this passively at $\sim 983\,K$ ($710\,^{\circ}C$) at $1\,s$ and $\sim 553\,K$ ($280\,^{\circ}C$) at one day, both below damage thresholds — so equation (11) is satisfied with no active cooling. The first-wall specific decay heat is $56.0\,W/kg$ at shutdown, falling to $1.22\,W/kg$ at one year and $2.4e-8\,W/kg$ at 100 years — orders of magnitude below the ~ 1–2%-of-thermal decay heat of a fission core [2,8]. We note the one caveat carried in the register: the $\leq 62\,W/kg$ figure is a one-year-cooled value, not a $t = 0$ bound.

Figure 6(b) places the stored-energy inventory in context. The breeder plasma stores only $16.06\,MJ$ ($\approx 3.8\,kg$ TNT-equivalent, serial ENV-A3) — a component-damage event, not an off-site hazard. The dominant stored energy is magnetic: $\sim 0.3\,GJ$ in the breeder coil set and $\sim 12.3\,GJ$ in the burner central-cell field (with the burner plasma thermal energy $\sim 10.2\,GJ$). Magnet energy is a quench/arc engineering hazard — managed by dump resistors and structural design — and is *radiologically inert*. The safety-relevant conclusion is unchanged: neither machine has a physical path to a runaway or a core melt.

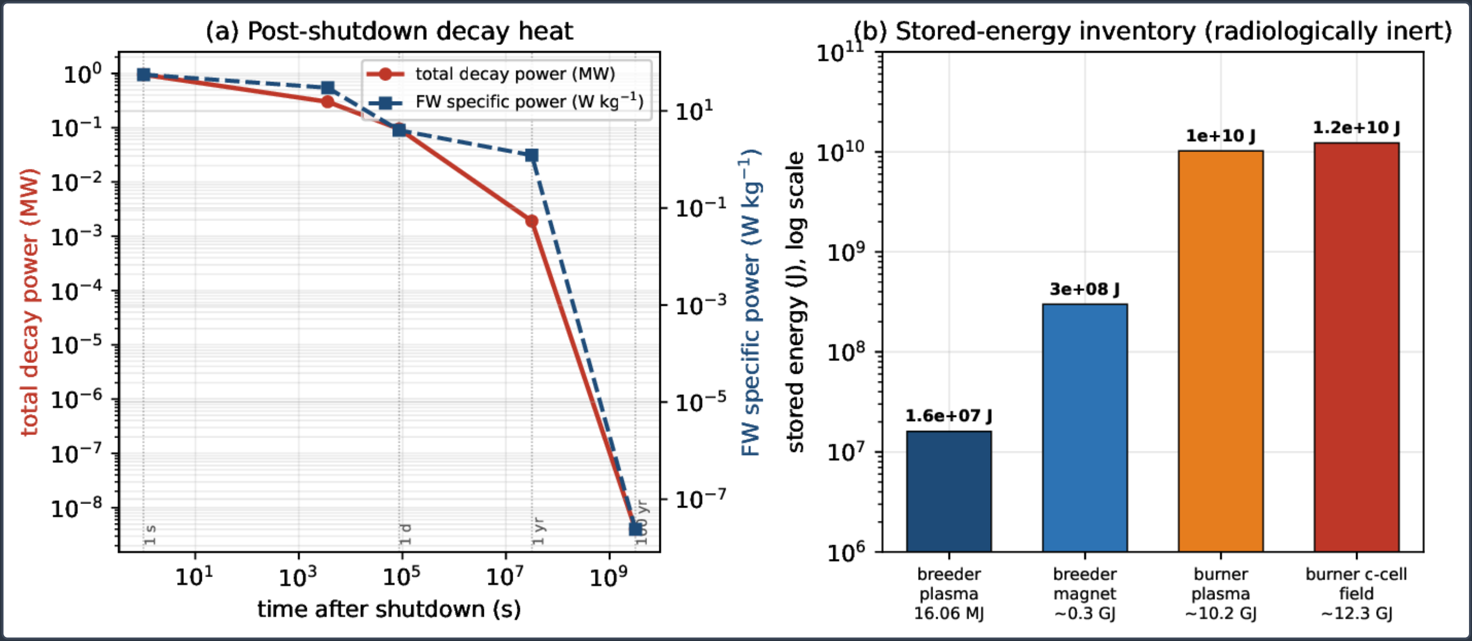

(a) Post-shutdown decay heat: total power (left axis, serial BR-L1-A9) and first-wall specific power (right axis, serial BR-L2-A23) versus time, from equation (10); the plasma-facing surface rejects this passively (equation 11). **(b)** Stored-energy inventory (log scale, serial ENV-A3): the plasma stores 16.06 MJ; the larger magnetic and burner-field energies are radiologically inert.

ACTIVATION, WASTE CLASS AND DECOMMISSIONING

Figure 7 shows the specific-activity trajectories of equation (12) from the R2S transport-plus-inventory calculation. The first wall (Eurofer-class) falls from $2.64e14\,Bq/kg$ at shutdown to $7.13e13\,Bq/kg$ at one year and $2.70e7\,Bq/kg$ at 100 years; the breeder zone follows the same trajectory (serial BR-L2-A23). The 10 CFR 61 Class-C index of equation (13) stays $\leq 2.6\times10^{-3}$ in both zones at all times, so nothing is GTCC and the structure is low-level waste [6,7]. The low-activation refractory high-entropy alloy set moves from intermediate-level ($\sim 6\times10^{14}\,\mathrm{Bq\,kg^{-1}}$, 51–$62\,\mathrm{W\,kg^{-1}}$ at one year) to low-level at ten years to clearable at 100 years, with a long-lived fraction of exactly zero, because the composition screen excludes Nb, Zr and Mo, whose ^{94}Nb/^{93}Zr products would otherwise fix a dirty alloy at intermediate level indefinitely (serial ENV-A2). No isotope in the qualified material set has a half-life beyond a century [25]. The one exception, stated honestly, is the copper centrepost: its impurity-limited activation tail is not clearable even at 1000 years, so the centrepost is handled as a scheduled *consumable* cartridge within the low-level-waste class rather than as clearable structure (serial BR-SX-11).

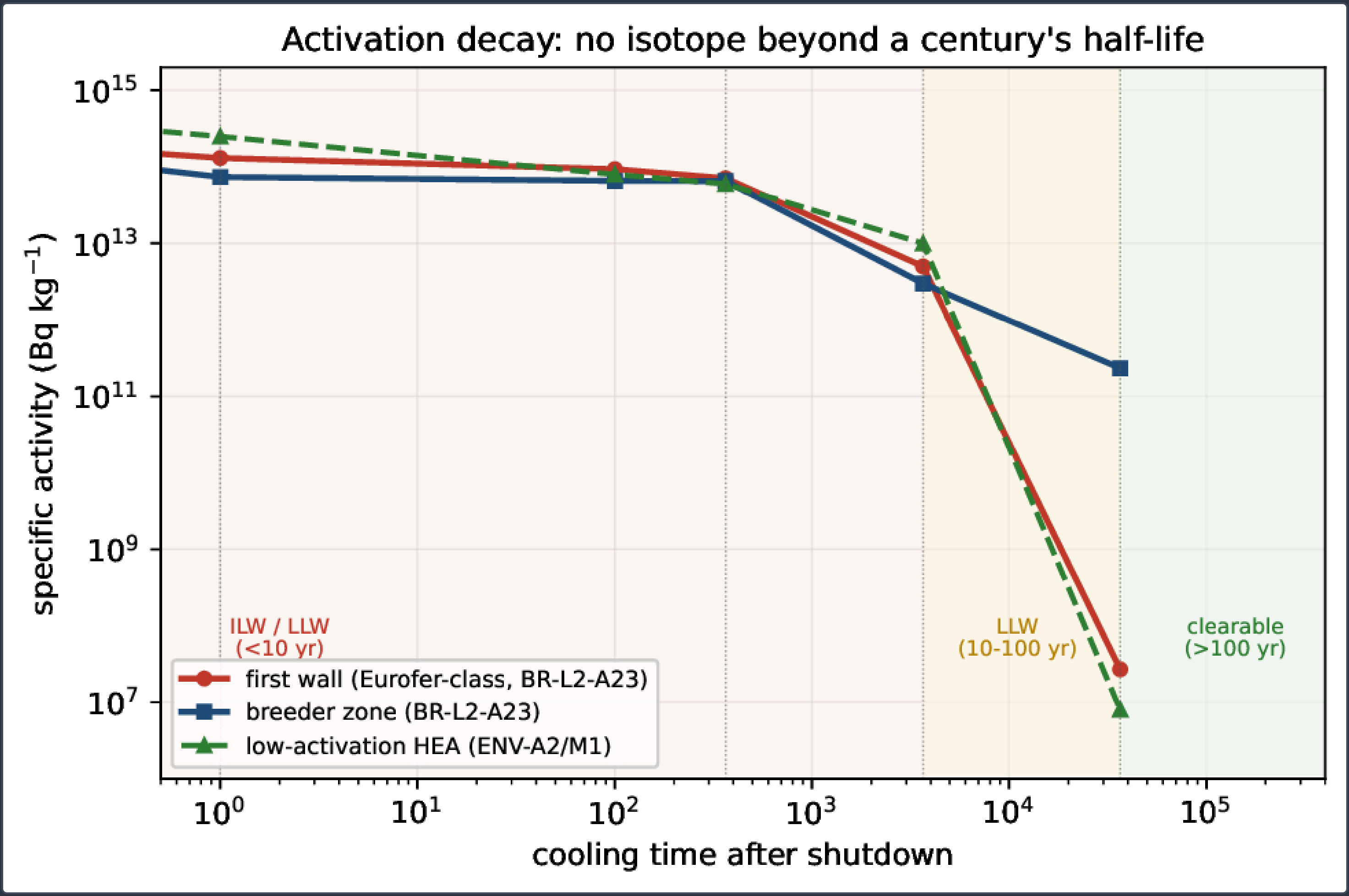

Activation decay (equation 12) of the first wall, breeder zone (serial BR-L2-A23) and low-activation HEA set (serial ENV-A2). Shaded bands mark the intermediate/low-level (<10 yr), low-level (10–100 yr) and clearable (>100 yr) regimes; no qualified isotope persists beyond a century.

PERMEATION CONTROL

The first-wall permeation source term (figure 8) is bounded by the diffusion–trapping calculation of §3.1. The steady flux is $5.16e14\,Tat/m^2s$ ($0.082\,g/m^2fpy$, 0.52–0.60% of the implanted flux) through the nominal $0.5\,mm$ W armour, scaling as $1/L_W$ so that a $3\,mm$ armour would reduce it to $\sim 1.0e14\,Tat/m^2s$ (serial BR-L2-A25). The permeation breakthrough time (analytic $L^2/6D$) is $\sim 190\,s$ at $600\,K$ and $\sim 30\,s$ at $800\,K$, so permeation reaches steady within minutes of a burn start and is a small, well-characterized loss term for the fuel-cycle balance — not a source-term surprise. Permeation-barrier coatings and the liquid-lithium wall chemistry [27] provide the required PRF ≈ 2000 that keeps the processing pool behind its barrier.

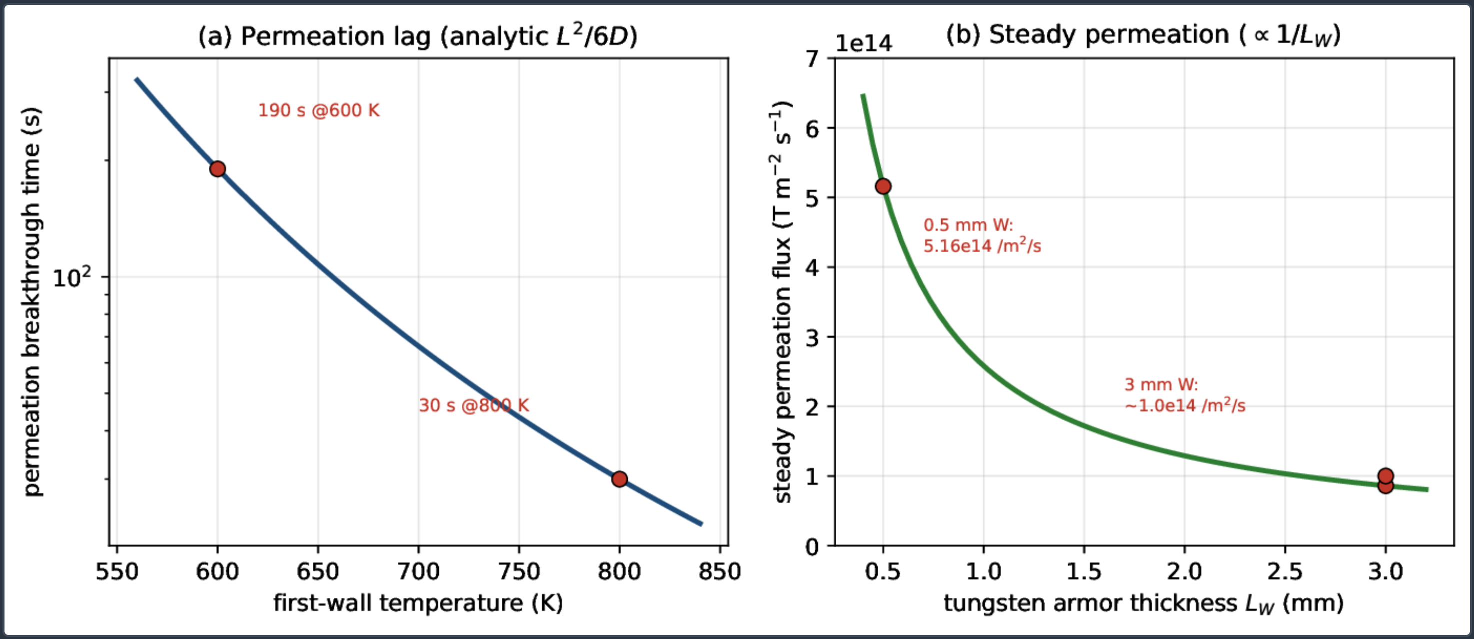

First-wall tritium permeation (serial BR-L2-A25). **(a)** Analytic breakthrough time $L^2/6D$ versus temperature (anchors $190\,s$ at $600\,K$, $30\,s$ at $800\,K$). **(b)** Steady permeation flux versus armour thickness, scaling as $1/L_W$ from $5.16e14\,Tat/m^2s$ at $0.5\,mm$.

ENVIRONMENTAL PROFILE

Operationally the plant emits zero direct CO_2: the D–T breeder products are He-4 + n and the D–^{3}He burner products are p + He-4, with no carbon in the fuel cycle (serial ENV-A1). The life-cycle greenhouse intensity sits in the published fusion/fission/wind class of 10–30 , dominated by embodied materials; at reference-class intensity ($\sim 40\,tonne$ steel and $\sim 90\,m^3$ concrete per MW(e) [21]) an $\sim 85\,MW$-class unit implies order 3–4 kt steel and ~8 kt concrete. Fuel demand is trivially met: per unit the breeder consumes $3.16\,kg/yr$ of deuterium and $17.1\,kg/yr$ of ^{6}Li ($\sim 225\,kg$ natural Li), against essentially unlimited resources (serial ENV-A4). We flag that the embodied-carbon figure is honest only at published-LCA-class fidelity until a bill-of-materials inventory is performed (§6).

§ 5

Discussion

THE SOURCE TERM AGAINST THE FUSION-SAFETY LITERATURE

The central quantitative message is that the mobilizable HTO source term, not the fusion power, sets the off-site consequence, and that the design keeps it small. Our realistic design-basis release ($4.8\,g$ HTO, $Q = 1.71e15\,Bq$) is comparable to the more severe ITER reference-event source terms, which the ITER safety analysis showed produce off-site doses below the French evacuation criteria [2,3]; our EPZ radii (table 3) reproduce that conclusion for a compact ST breeder with an independent dispersion-and-dose chain. The favourable factor here is the smaller absolute inventory: a sub-$100\,MW$ breeder with direct internal recycling carries a mobilizable pool of grams, not the tens-of-grams-to-kilograms range of a GW-class D–T plant [1,5]. The burner is more favourable still — its $\sim 3.6\,g$ mobile HTO inventory (serial MV-CX-29) makes urban and forward-base siting a dispersion problem with almost no source to disperse, consistent with the neutron-lean siting analysis [29].

NO MELTDOWN, QUANTITATIVELY

The walk-away result is qualitatively identical to, and quantitatively consistent with, the inherent-safety case established for DEMO and ARIES-class plants: decay heat orders of magnitude below fission, no critical mass, and passive coolability [2,5]. The distinguishing number here is the plasma stored energy of only $16.06\,MJ$ — a compact, sub-$100\,MW$ device simply has little to release — and the explicit radiative balance of equation (11) satisfied at $\leq 710\,^{\circ}C$. The honest caveat is that the largest stored-energy term is magnetic (order $0.3\,GJ$ breeder, $12.3\,GJ$ burner field): this is a real engineering hazard, but it is radiologically inert and is addressed by quench protection, not by emergency planning.

WASTE AGAINST THE CLEARANCE LITERATURE

The activation result — all structural streams at or below Class C, no isotope beyond a century, long-lived fraction zero for the qualified alloys — matches the low-activation-materials programme goals of the fusion community [8,6,7] and is achieved by the same lever they identify: excluding the niobium-, zirconium- and molybdenum-bearing elements whose activation products carry the long-lived tail. The copper-centrepost exception is a genuine, quantified deviation, and the design answer — treat it as a scheduled consumable within the low-level class rather than as clearable structure — is the honest one; the decommissioning consequence is developed in the companion activation/waste-routing paper [25].

THE REGULATORY CONSEQUENCE

The chain assembled here is the technical basis for a light-touch licensing posture. Because the accident source term is a small mobilizable tritium inventory rather than a large fission-product inventory, and because the resulting EPZ collapses toward the site boundary under all but the most conservative assumptions, the plant does not present the off-site consequence profile that drives 10 CFR 50/100 power-reactor licensing and its $16\,km$ EPZ [20]. The byproduct-material licensing thesis — that a compact ST breeder licenses under NRC 10 CFR Part 30 rather than Part 50 — is developed in the companion licensing paper [30]; the present source-term, dispersion and EPZ results are its quantitative underpinning.

§ 6

Limitations

This is a design-basis safety analysis, not a licensed safety analysis report, and three honest bounds apply. First, the dispersion model is a bounding Gaussian plume: it takes no credit for plume rise, building-wake dilution, dry or wet deposition, or plume depletion, and assumes the released tritium is fully oxidized to HTO — every one of these choices is conservative (raises the computed dose), but a site-specific consequence assessment with a validated dispersion code and real meteorology would be required for a license. Second, the accident source term is a barrier-attenuated fraction of a computed standing inventory; the release fractions f_R are parametric bounds, not the output of a plant-specific fault-tree and MELCOR-class mobilization analysis, which is the natural next step. Third — the one genuinely open engineering item — the embodied-carbon and materials life-cycle figure is supportable only at published-LCA-class fidelity until a bill-of-materials inventory is performed for the actual Kronos design; no local tool computes it today (serial ENV-A1).

§ 7

Conclusion

We have assembled an end-to-end environmental and safety chain for the Hyperion compact ST breeder, from a frozen tritium inventory through an explicit atmospheric-dispersion and dose calculation to an emergency-planning-zone radius, and closed the secondary hazards at the same design point. The dominant hazard is the mobilizable tritium inventory, which the design keeps to a $4.8\,g$ blanket pool and a barrier-confined $675\,g$ processing inventory; the resulting EPZ is sub-kilometre for the realistic design-basis release and collapses inside the site boundary under typical weather, always far within the $16\,km$ generic power-reactor zone. There is no meltdown mechanism by construction: the plasma stores only $16.06\,MJ$, the fusion rate quenches on any loss of confinement, and post-shutdown decay heat is passively rejected below damage temperatures. Activation keeps all structural streams at or below Class C with no isotope beyond a century's half-life, the copper centrepost handled honestly as a scheduled consumable; the plant emits zero direct CO_2 and sits in the 10–30 life-cycle class. Every headline number is a frozen anchor in the de-risking register, and the single open item — a bill-of-materials life-cycle inventory — is stated, not hidden. The safety case is bounded, not asserted.

Acknowledgments tocsectionAcknowledgments Part of the Kronos Fusion Energy 2026 design series. The authors thank the Kronos physics de-risking programme for the frozen result set underlying every quantitative claim, and the NVIDIA GPU HPC campaign for the transport, activation and permeation computations.

Reproducibility. Every headline quantity in this paper is a frozen anchor (the cited serials) in the Kronos Physics De-Risking Register (doi:10.5281/zenodo.22133057) and is regenerable from the archived transport, inventory, permeation and fuel-cycle inputs together with the figure-generation script deposited with this paper. This paper is archived at doi:10.5281/zenodo.22645754 and its official version is at https://www.kronosfusionenergy.com/publications/inherent-safety-and-environmental-case.html. No result depends on unpublished or proprietary data, and no economic quantity enters the analysis.

Data availability tocsectionData availability The tritium inventory ledger, source-term family, dispersion/dose curves, EPZ radii, decay-heat and stored-energy values, activation trajectories and permeation results used for figures 2–8 are archived with the deposit at doi:10.5281/zenodo.22645754, which references the Kronos 2026 series and the register [22]. All quantitative values trace to the register by the serial identifiers cited inline. No economic analysis is part of the public deposit.

Competing interests tocsectionCompeting interests Provisional patent applications relating to aspects of this work have been filed.

tocsectionReferences

APPARATUS

Portfolio, People & Record

The intellectual-property estate, the people who built it, the limitations that gate it, and the sources it rests on.

1	4	40	27
GRANTED PATENT	2026 PROVISIONALS	TEAM MEMBERS	2022 PROVISIONALS

INTELLECTUAL PROPERTY

The patent portfolio

The estate spans a granted high-field magnet patent, pending utility and 2026 provisional filings that map to the two products, a digital-twin control provisional, a registered trademark application, and the original 2022 provisional family. Every patentable disclosure in the five-paper arXiv drop was protected **before** publication: the breeder and burner provisionals were filed 1–2 August, and a publication-gap omnibus filing the evening before the drop swept up the DEC, plasma-control, and REBCO-winding matter of the three otherwise-unprotected papers. Patent numbers and application serials are matters of public record; claim scope is summarised, not reproduced.

GRANTED & PENDING UTILITY

US 12,009,112	High-field tilted graded-REBCO magnet architecture (KRONO-002A) · *app. 17/878,550*	GRANTED
US 17/878,507	Core device / method (KRONO-001A) · *utility*	PENDING

2026 PROVISIONAL FILINGS — MAPPED TO THE PRODUCTS

64/124,209	Hyperion — spherical-tokamak tritium / helium-3 foundry · *breeder · filed Aug 2026*	FILED
64/124,220	Aegis / MetroVolt — synchrotron-cutoff, fuel-selection & plug-winding · *generator · filed Aug 2026*	FILED
64/115,167	KRONOS-CTRL digital-twin plant control · *provisional · filed Jul 2026*	FILED
64/005,440	Integrated spherical-tokamak fusion architecture · *early integrated-architecture filing · filed Mar 2026*	FILED
64/105,530	Negative-triangularity spherical-tokamak architecture · *foundational ST filing · filed Jul 2026*	FILED
64/128,097	Publication-gap omnibus — quasineutral two-species expander DEC · provenance-gated / latency-split plasma control · as-built high-field winding & conductor architecture · *filed 7 Aug 2026, the evening before the arXiv drop*	FILED

TRADEMARK & ORIGIN

FTK-98801894	Kronos Fusion Energy — trademark application	FILED
KR-2022-*	Original provisional family (KR-2022-00001 … 00027) · *27 filings, 2022*	PRIORITY

The narrow, defensible magnet novelty — the specific conductor and the digital-twin winding optimisation, not high-field REBCO as a category — is the commercial core that can earn ahead of any Q > 1 milestone, with markets in fusion magnet supply, MRI/NMR, accelerators, and proton therapy. The claim is scoped honestly: the high field is a *system field* result, not a stand-alone-coil record; the small-bore plug coil is structurally infeasible as a bare winding but resolved by a stress-managed structural shield (feasible-pending-FEA); and the winding-tape experiment returned a *null result*. The value is the method, not a field record.

THE TEAM

Founding partners, board, advisors & auditors

Kronos is built by a bench of advanced-fuel-fusion, high-field-magnet, direct-conversion, and materials specialists, with a board and operations team drawn from defense, national laboratories, and industry. Dates are shown as ranges; where a tenure has ended or is term-ending, the range says so.

FOUNDING PARTNERS — SCIENCE

Dr. Gerald Kulcinski
Co-Founder · Helium-3 & Advanced-Fuel Fusion
UW–Madison · 2023–Present

Dr. Carl Weggel
Chief Scientist / S.M.A.R.T. Design
MIT Alcator Program · 2022–Present

Dr. Robert J. Weggel
Magnetic Field Design
MIT Magnet Lab · 2022–Present

BOARD

Priyanca Ford
Founder & CEO · Executive Board
2022–Present

Bandel Carano
Finance / Strategy
Oak Investment Partners / Stanford · 2025–2026

Patrick Schweiger
Fusion Device Engineering
Oklo / CFS / TerraPower · 2025–Present

SCIENTIFIC ADVISORS

Dr. Steven O. Dean
Fusion Policy & History
DOE / Fusion Power Associates · 2025–Present

Dr. Patrick H. Diamond
Plasma Turbulence & Transport
UC San Diego · 2025–Present

Dr. Jack J. Dongarra
HPC & Numerical Algorithms
Turing Award · 2025–Present

Dr. Nasr M. Ghoniem
Chief Material Scientist
UCLA · 2025–Present

Dr. Siegfried Glenzer
Plasma Physics & Laser Fusion
Stanford / SLAC · 2022–Present

Dr. David A. Hammer
Pulsed-Power Fusion
Cornell · 2025–Present

Dr. Donald A. Spong
Plasma Theory & Confinement
ORNL · 2025–Present

Dr. Curtis Smith
Risk Assessment & Nuclear PRA
MIT / Idaho National Lab · 2025–Present

RADM (Ret.) David Goggins
Naval Engineering & Power-Plant Design
U.S. Navy · 2023–2026

Dr. Konstantin Batygin
Mathematician
Caltech · 2022–2025

Dr. Ruben Fair
Magnet Design / ITER Liaison
PPPL / Jefferson Lab · 2022–2025

Dr. Paul S. Weiss
Materials & Nanotechnology
UCLA · 2022–2025

SCIENTIFIC AUDITORS

Dr. Wilfred A. Cooper
Plasma Equilibrium Theory
EPFL / Swiss Plasma Center · 2025–Present

Dr. Ahmed Hassanein
Plasma–Material Interactions
Purdue / Argonne · 2025–Present

Dr. Patrick E. Hopkins
Extreme Thermal Materials
U. of Virginia · 2025–Present

Dr. Peter Hosemann
Materials Joining & Structural Integrity
UC Berkeley · 2025–Present

Dr. Travis W. Knight
Advanced Nuclear Fuels & Systems
U. of South Carolina · 2025–Present

Dr. Philippe Lebrun
Cryogenics & Magnet Cooling
CERN · 2025–Present

Dr. Nitendra Singh
Nuclear Safety & Fuel Cycle
ITER · 2025–Present

Dr. Guido Van Oost
Magnetic Confinement & Fusion Systems
Ghent University · 2025–Present

Dr. Gary S. Was
Radiation Materials & Structural Integrity
U. of Michigan · 2025–Present

Dr. Ray Sedwick
Direct Energy Conversion
U. of Maryland · 2025

OPERATIONS

Michael Laughlin
Chief Operating Officer
2022–Present

Martin Owens
Chief Strategy Officer
LANL / GE Hitachi · 2022–Present

MG (Ret.) Paul Pardew
Chief Contracting Officer
Army Contracting Command · 2022–Present

David Beck
Fusion Commercialization
U.S. Space Force · 2024–Present

Sushma Bhatia
Environmental & Legislative
Google · 2022–Present

Michael De Frenza
Technology Licensing
2023–Present

MG (Ret.) Robin L. Fontes
Cybersecurity & Defense
Army Cyber Command · 2022–Present

Vijay Gehani
Supply Chain & Components
INOX India · 2024–Present

Jon Michel Greenwood
IT & AI Infrastructure
Live Nation · 2023–Present

Brian C. O'Neill
National Security
CIA / ODNI · 2022–Present

Gen. (Ret.) Gustave F. Perna
DoD Liaison
Operation Warp Speed · 2022–2023

Andrea Romero
Marketing Lead
2022–Present

Legal counsel is retained; those roles are held on the internal roster and are not listed here.

SOURCES

References

1 M Abdou *et al*, Physics and technology considerations for the deuterium–tritium fuel cycle and conditions for tritium fuel self-sufficiency, *Nucl. Fusion* **61** 013001 (2021). doi:10.1088/1741-4326/abbf35

2 N Taylor *et al*, Resolving safety issues for a demonstration fusion power plant, *Fusion Eng. Des.* **124** 1177 (2017).

3 B J Merrill, P W Humrickhouse and R L Moore, A recent version of MELCOR for fusion safety applications, *Fusion Eng. Des.* **85** 1479 (2010).

4 J E Menard *et al*, Fusion nuclear science facilities and pilot plants based on the spherical tokamak, *Nucl. Fusion* **56** 106023 (2016). doi:10.1088/0029-5515/56/10/106023

5 D Maisonnier *et al*, Power plant conceptual studies in Europe, *Nucl. Fusion* **47** 1524 (2007).

6 L El-Guebaly and S Malang, Toward the ultimate goal of tritium self-sufficiency: technical issues and requirements imposed on ARIES advanced power plants, *Fusion Eng. Des.* **84** 2072 (2009).

7 M Zucchetti *et al*, The back-end of the fusion materials cycle: recycling and clearance of activated materials, *Fusion Sci. Technol.* **52** 597 (2007).

8 M R Gilbert *et al*, Activation, decay heat, and waste classification of candidate fusion materials, *Nucl. Fusion* **57** 046015 (2017). doi:10.1088/1741-4326/aa5bd7

9 J-C Sublet, J W Eastwood, J G Morgan, M R Gilbert, M Fleming and W Arter, FISPACT-II: an advanced simulation system for activation, transmutation and material modelling, *Nucl. Data Sheets* **139** 77 (2017).

10 P K Romano, N E Horelik, B R Herman, A G Nelson, B Forget and K Smith, OpenMC: a state-of-the-art Monte Carlo code for research and development, *Ann. Nucl. Energy* **82** 90 (2015). doi:10.1016/j.anucene.2014.07.048

11 R A Causey, Hydrogen isotope retention and recycling in fusion reactor plasma-facing components, *J. Nucl. Mater.* **300** 91 (2002).

12 R Delaporte-Mathurin *et al*, Finite-element analysis of hydrogen transport and trapping in fusion materials with FESTIM, *Int. J. Hydrogen Energy* **63** 786 (2024).

13 F Pasquill, The estimation of the dispersion of windborne material, *Meteorol. Mag.* **90** 33 (1961).

14 F A Gifford, Use of routine meteorological observations for estimating atmospheric dispersion, *Nuclear Safety* **2** 47 (1961).

15 G A Briggs, *Diffusion Estimation for Small Emissions*, Atmospheric Turbulence and Diffusion Laboratory report ATDL-79 (NOAA, 1973).

16 S R Hanna, G A Briggs and R P Hosker, *Handbook on Atmospheric Diffusion*, DOE/TIC-11223 (US Department of Energy, 1982).

17 International Commission on Radiological Protection, Age-dependent doses to members of the public from intake of radionuclides: Part 5, compilation of ingestion and inhalation dose coefficients, *ICRP Publication 72*, Ann. ICRP **26**(1) (1996).

18 International Commission on Radiological Protection, Compendium of dose coefficients based on ICRP Publication 60, *ICRP Publication 119*, Ann. ICRP **41**(Suppl.) (2012).

19 US Environmental Protection Agency, *PAG Manual: Protective Action Guides and Planning Guidance for Radiological Incidents*, EPA-400/R-17/001 (2017).

20 US Nuclear Regulatory Commission, Emergency planning and preparedness for production and utilization facilities, 10 CFR 50.47 and Appendix E; NUREG-0396 basis for the 10-mile plume-exposure EPZ (1978).

21 P F Peterson, H Zhao and G Petroski, Metal and concrete inputs for several nuclear power plants, University of California Berkeley report UCBTH-05-001 (2005).

22 P I Ford, *The Physics De-Risking Register: Gate-by-Gate Evidence, Independently Re-Run and Stamped*, Kronos Fusion Energy 2026 series. doi:10.5281/zenodo.22133057

23 P I Ford, *Hyperion as a Strategic-Materials Platform: Gain, Tritium Breeding, He-3 Co-Production, and 14 MeV Neutron Output from a Compact Spherical-Tokamak*, Kronos Fusion Energy 2026 series. doi:10.5281/zenodo.22645691. kronosfusionenergy.com/publications/breeder.html

COLOPHON

How this document was made

The Kronos Fleet — Combined Editorial, 2026 is set in **Fraunces** (display), **Gelasio** (text), and **IBM Plex Mono** (data & equations), carried forward from the Kronos editorial design system.

The figures are rendered at 300 dpi from the deposited generator scripts; the document is composed as a single self-contained file with embedded fonts and imagery, paginated to US Letter, and rendered to PDF through a headless Chromium engine in matched light and dark editions.

Every headline quantity carries an evidence class; withdrawn and restated values are marked as such. Nothing herein is frozen beyond the founder-approved Tier-A set.

Explore it live — turn the interactive 3-D model, run the deposited solvers in the physics validator, and watch the companion film series.

LEGAL NOTICE

Notice, status, and distribution

Conceptual design & simulation study. This document reports a conceptual design and simulation study. It is not a construction commitment, a safety-analysis report, a regulatory filing, or an offer of securities. Forward-looking statements — schedules, costs, market sizes, and performance — are estimates subject to the limitations set out in the Simulations part and may change.

Numbers and their classes. Quantities are reported with evidence classes and case labels; modelled, assumed, and requirement-class values are identified as such and are not to be quoted without their labels.

Public edition. This edition carries the physics and design only; all financial, funding, and defense-commercial content has been removed for public distribution. The scientific text corresponds to the arXiv and journal submissions.

THE 2026 KRONOS SERIES

One programme, many papers

This editorial is one paper in the Kronos 2026 series — a real fusion company's complete, reproducible physics record for a spherical-tokamak breeder and its low-neutron D–^{3}He tandem-mirror burners. Every headline number is a frozen anchor in the Physics De-Risking Register.

Explore the whole programme: the De-Risking Register, the interactive 3-D model, and the physics validator.

KRONOS FUSION ENERGY

Environmental Profile, Accident Analysis and the Tritium Safety Case for a Multi-Kilogram Breeder Plant: Source Terms, Dispersion and Emergency-Planning-Zone Sizing

A real fusion company building real machines. Explore the science, live.

Zenodo · doi:10.5281/zenodo.22645754

Read on kronosfusionenergy.com

The Physics De-Risking Register